

On the possibility of extending the Nore-Frenkel
generalized law of correspondent states to
non-isotropic patchy interactions.

Giuseppe Foffi* and Francesco Sciortino†

* Institut Romand de Recherche Numérique en Physique
des Matériaux (IRRMA) and Institute of Theoretical Physics (ITP),
Ecole Polytechnique Fédérale de Lausanne (EPFL),
CH-1015 Lausanne, Switzerland

†Dipartimento di Fisica and INFN-CNR-CRS Soft,
Università di Roma *La Sapienza*, P.le A. Moro 2, 00185 Roma, Italy

July 18, 2021

Abstract

Colloidal systems (and protein solutions) are often characterized by attractive interactions whose range is much smaller than the particle size. When this is the case and the interaction is spherical, systems obey a generalized law of correspondent states (GLCS), first proposed by Noro and Frenkel [J.Chem.Phys. 113, 2941 (2000)]. The thermodynamic properties become insensitive to the details of the potential, depending only on the value of the second virial coefficient B_2 and the density ρ . The GLCS does not generically hold for the case of non-spherical potentials. In this Letter we suggest that when particles interact via short-ranged small-angular amplitude patchy interactions (so that the condition of only one bond per patch is fulfilled) it is still possible to generalize the GLCS close to the liquid-gas critical point.

Keywords: Colloids, Second Virial Coefficient, Proteins interactions, Short-ranged attractive attractions.

In colloidal and in protein systems, the interaction potential is often short-ranged, i.e. small as compared to the particle size. The small-range interaction brings some peculiar behaviour both on the system thermodynamics and on the dynamics. For example, the gas-liquid phase separation becomes metastable with respect to crystallization [1] (and hence a proper equilibrium liquid phase is missing). In addition, for very short ranges, the kinetic arrest (glass) line becomes reentrant and two different glass phases appear [2, 3]. The presence of short-range attractions is also invoked to explain the so-called “crystallization slot” in the phase diagram of globular proteins [4].

A common property unifies all spherically symmetric short ranged attractive potentials, independently from their actual shape. Indeed, Noro and Frenkel [5] showed that the thermodynamical properties of systems interacting with short-range attractive potentials are all equivalent if scaled by the proper variables, i.e. they obey a generalized law of correspondent states (GLCS). They showed that the virial coefficient can be used as scaling variable for the strength of the interaction. Recently, the GLCS has been shown to arise from the fact that, due to the short-range of the interaction, each interacting pair of particles (a bond) contributes independently and equally to the partition function [6].

The above considerations are valid for centrosymmetric potentials and can not be straightforwardly extended to non-spherical cases [7, 8], i.e. when interactions are patchy and strongly directional. In the case of molecular fluids, patchy interactions are relevant in network-forming systems, like silica [9, 10] and water [11, 12] and in all associating fluids [13, 14] in which the hydrogen bond plays an important role. For colloidal systems, this interest is justified by recent advances in the synthesis and characterization of patchy particles [15, 16, 17, 18] or functionalized colloidal particles [19]. For what concern proteins, it is well established that the interactions are intrinsically directional [20, 21, 22] and that their description in term of isotropic potentials represents only a first-order approximation.

Recent progress in understanding the thermodynamic of patchy colloidal particles has been based on application of the thermodynamical perturbation theory developed by Wertheim [23]. The theory, which does not account for the geometry of the patches, assumes that each patch acts as an independent interacting unit. In addition, the theory neglects the possibility of close-loops of bonds. Despite these approximations, several predictions of the theory have been numerically confirmed [13, 24, 25]. It has been shown that (for the case of patchy interactions) the number of *independent* interacting patches (the valence) is the key ingredient in controlling the phase diagram of the system. On lowering the valence, the liquid-gas critical point shifts to smaller and smaller densities, so that liquid states of vanishing density (empty liquids) become accessible [24]. The Wertheim expression for the bonding free-energy is a function only of the bond probability and of the valence. In this respect, the theory suggests that systems with the same valence should behave similarly, if the bond probability is the same. Since the bond probability is related to the chemical bonding constant [13, 25], and since for large attraction strengths the chemical constant is proportional to the second virial coefficient [20], the Wertheim theory suggests

that universality based on the virial scaling can be recovered also in the case of patchy interactions when valence is preserved.

To address the issue of a possible generalization of the Noro-Frenkel scaling we have extended the investigation concerning the location of the critical point for the patchy model introduced by Kern and Frenkel [7], for several values of the attraction range and of the width of the patchy attractive region. The choice of this potential is motivated by the fact that angular and radial properties can be independently modified. More precisely, the two body potential is defined as:

$$u(\mathbf{r}_{ij}) = u^{sw}(r_{ij})f(\{\Omega_{ij}\}) \quad (1)$$

where $u^{sw}(r_{ij})$ is an isotropic square well term of depth u_0 and attractive range $\sigma + \Delta$ and $f(\{\Omega_{ij}\})$ is a function that depends on the orientation of the two interacting particles $\{\Omega_{ij}\}$. The diameter of the particles and the depth of the square well has been chosen as units of length and energy respectively, i.e. $\sigma = 1$ and $u_0 = 1$. Each particle is characterized by M identical patches. A patch α is defined as the intersection of the surface of the sphere with a cone with half-opening angle θ that has the vertex in the center of the particle and it has the axis directed toward the direction $\hat{\mathbf{u}}_\alpha$. The angular function $f(\{\Omega_{ij}\})$ is defined as

$$f(\{\Omega_{ij}\}) = \begin{cases} 1 & \text{if} \\ 0 & \text{else} \end{cases} \left\{ \begin{array}{l} \hat{\mathbf{r}}_{ij} \cdot \hat{\mathbf{u}}_\alpha > \cos \theta \\ \text{and} \\ \hat{\mathbf{r}}_{ij} \cdot \hat{\mathbf{u}}_\beta > \cos \theta \end{array} \right. \begin{array}{l} \text{some patch } \alpha \\ \text{on particle } i \\ \\ \text{some patch } \beta \\ \text{on particle } j \end{array} \quad (2)$$

where $\hat{\mathbf{r}}_{ij}$ is the direction of the vector that joins the centers of the two interacting particles and α (β) some patch belonging to the particle i (j). In practice two particles interact attractively if, when they are within the attractive distance $\sigma + \Delta$, two patches are properly facing each other. When this is the case, the two particles are considered bonded. Decreasing Δ reduces the range of the attraction whereas reducing θ diminishes the angular size of the patches. In the limit $\Delta \rightarrow 0$ the model goes toward the patchy Baxter limit. In the limit $\cos \theta \rightarrow 1$, the patch goes to the point limit.

In the present work we focus on $M=3$, $M=4$ and $M=5$ patches, located on the surface of the particle as shown in the cartoon of Fig. 1. Differently from previous studies [7], we consider values of Δ and θ such that, due to steric reasons, each patch is involved simultaneously in only one pair interaction, i.e. those values fulfilling the condition $\sin \theta > \frac{\sigma^2}{2(\sigma+\Delta)^2}$. Under this single-bond per patch condition, the number of patches coincides also with the maximum number of possible bond per particle.

The Kern-Frenkel potential posses an analytical expression for the second virial coefficient:

$$\frac{B_2}{B_2^{HS}} = 1 - \chi^2((1 + \Delta)^3 - 1)(e^{1/T} - 1) \quad (3)$$

where $\chi = M \frac{1 - \cos(\theta)}{2}$ is the percentage of surface covered by the attractive patches and the temperature is measured in reduced units, i.e. $k_B = 1$. Here B_2^{HS} is the hard-sphere component of the virial coefficient. To calculate the location of the gas-liquid critical point we perform grand canonical Monte Carlo (GCMC) simulations [26], complemented with histogram reweighting techniques to match the distribution of the order parameter $\rho - se$ with the known functional dependence expected at the Ising universality class critical point [27]. Here e is the potential energy density, ρ the number density and s is the mixing field parameter. We did not performed a finite size study, since we are only interested in the trends with the range Δ and the angular size of the patches θ . We have studied systems of size $L = 6$ for $M = 4$ and 5 and $L = 7$ for $M = 3$, where L is the side length of the cubic simulation box. For each studied M — using the methods described in [28] — we calculated the critical temperature T_c and density ρ_c for values of Δ between 0.119 and 0.01 (at fixed $\cos \theta = 0.92$) and for $\cos \theta$ between 0.895 and 0.99 (at fixed $\Delta = 0.119$). The results are summarized in Table 1.

We start by analyzing the results as a function of Δ , at fixed $\cos \theta = 0.92$. Fig. 2 shows that T_c decreases with Δ while ρ_c increases. The Δ dependence of ρ_c can be conveniently described by $\rho_c(\Delta) = \rho_c(0)/(1+0.5\Delta)^3$, a functional form which suggests that ρ_c would be constant if measured using as unit of length the average distance between two bonded particles ($1 + 0.5\Delta$). The resulting $\rho_c(0)$ extrapolated value provides an estimate of the corresponding patchy Baxter model ρ_c . Fig. 2-(a) shows also that the T_c dependences are apparently well described by iso- B_2 lines. Each M is characterized by a different B_2 value, enforcing the existence of a GLCS for each valence. As a confirmation, we evaluate the values of B_2/B_2^{HS} at the critical point for the patchy particle model studied in Ref. [24]. The resulting values for $M = 3, 4$ and 5 are respectively $B_2/B_2^{HS} = -28.12, -4.95$ and -2.78 , very similar to the values reported in the present study. We also note that the B_2 differences between different M values are much larger than the variation with Δ at constant M . Hence at a zero-th order approximation, when the repulsive part of the potential is complemented by localized patchy interactions, B_2 can be considered as a scaling variable of a GLCS in the single-bond per patch condition.

A closer look to the actual B_2 values (see Table 1) shows that a small trend in the B_2 values is present, which is hidden in the logarithmic transformation relating B_2 to T (see Eq. 3). Still, the B_2 differences between different M values are much larger than the variation with Δ at constant M . This suggests that, at a zero-th order approximation, B_2 can be considered as a scaling variable of a GLCS in the single-bond per patch condition. Thus, provided that the geometry of the patches is such that their number coincides with the maximum valence, B_2 carries the information on the valence of the patchy interaction potential. These results suggest that, statistically, configurations with the same Boltzmann weight are generated under an isotropic scaling (to change the inter-particle distances preserving the same bonding pattern) and a simultaneous change of both Δ and T such that B_2 remains constant. It is interesting to

observe that the GLCS for the isotropic square well is fulfilled for values of the range smaller than 0.05 [6, 29], whereas for the three models discussed here GLCS appears to hold for longer ranges.

Fig. 3 shows T_c and ρ_c , this time at $\Delta = 0.119$, as a function of $\cos\theta$. For values of $\cos\theta$ larger than the one reported in the figure, crystallization is observed within the simulation time, preventing the possibility of evaluating the critical parameters. This effect suggests that the liquid-gas critical point is metastable, as in the case of spherical short-range potentials. The observation of crystallization inform us already that on reducing θ , some bonding patterns acquires a larger statistical weight. Indeed, differently from the previous case, small deviations from a GLCS are observed in T (see lines Fig. 3-(a)) and not only in B_2^c . We attribute these deviation to the fact that by changing the angular part of the potential, the statistical relevance of specific bonding patterns varies. In other words, it is not possible to vary the orientation of the particles to preserve the bonding on changing θ , i.e. it is not possible to perform the operation equivalent to rescaling the distances to preserve the bonding pattern on changing Δ . We expect that the breaking of the scaling will be enhanced at state points far from the critical region where an extensive bonding pattern is present, i.e. low T and large ρ . Concerning the θ dependence of ρ_c , we note that it increases with $\cos\theta$, for the case $M = 5$ and $M = 4$ while it weakly decreases for $M = 3$. We have no clear arguments for interpreting the $\rho_c(\theta)$ trends, except for the fact that the observed dependence (more significant for $M = 4$ and $M = 5$), suggests a non-trivial coupling between the angular correlation induced by bonding and the density. For these two M values, small bonding angles appear to require smaller average distances between next-nearest neighbor particles implying larger densities.

The argument behind the quasi-validity of the GLCS for each M class are based on the fact that the relevant role is played by the bonding pattern [6], which is supposed to be statistically identical for all members of the class along corresponding states. Hence, the number of bonds at the critical point should be similar. To double check this statement we also report in Table 1 the bond probability p_b^c , defined as the potential energy at the critical point normalized by the energy of the fully bonded system. Such quantity is indeed constant for each M value, in agreement (and strongly supporting) the possibility of defining a different GLCS for each valence class. We also note that, within each M class, the variation of p_b^c are smaller than the one of B_2 , suggesting that the bond probability may result in a better scaling variable than B_2 . A small trend in p_b^c is only observed in the θ dependence. We also note that this observation is in agreement with the Wertheim theory [23] and with the identification of the bond free energy as the appropriate scaling variable for the spherical case [6].

In summary, we have provided evidence that different short-ranged non-spherical potentials, but with the same number of single-bond patches, essentially obey a GLCS. The condition of a single-bond per patch requires that both the attraction range and the angular size of the patches are small. Breakdowns of the GLCS can be expected for potentials which differ in their angular part, especially for very small angular sizes ($\cos\theta \rightarrow 1$), since — in conditions of

extensive bonding — the statistical weight of closed loops of bonds becomes significantly affected by the angular patch size.

We acknowledge support from Swiss National Science Foundation Grant No. 99200021-105382/1 (GF) and MIUR PRIN (FS).

References

- [1] Gast, A. P.; Russell, W. B.; Hall, C. K. *J. Colloid Interface Sci.* **1983**, *96*, 251.
- [2] Sciortino, F. *Nat. Mater.* **2002**, *1*, 145.
- [3] Dawson, K. A.; Foffi, G.; Fuchs, M.; W. Gotze; Sciortino, F.; Sperl, M.; Tartaglia, P.; Voigtmann, T.; Zaccarelli, E. *Phys. Rev. E* **2001**, *63*, 11401.
- [4] ten Wolde, P. R.; Frenkel, D. *Science* **1997**, *277*, 1975.
- [5] Noro, M.; Frenkel, D. *J. Chem. Phys.* **2000**, *113*, 2941.
- [6] Foffi, G.; Sciortino, F. *Phys. Rev. E* **2006**, *74*, 050401.
- [7] Kern, N.; Frenkel, D. *J. Chem. Phys.* **2003**, *118*, 9882.
- [8] Charbonneau, P.; Frenkel, D. *J. Chem. Phys.* **2007**, *126*, 196101.
- [9] Vega, C.; Monson, P. *J. Chem. Phys.* **1998**, *109*, 9938.
- [10] De Michele, C.; Gabrielli, S.; Tartaglia, P.; Sciortino, F. *J. Phys. Chem B.* **2006**, *110*, 8064.
- [11] Kolafa, J.; Nezbeda, I. *Mol. Phys.* **1987**, *61*, 161.
- [12] De Michele, C.; Tartaglia, P.; Sciortino, F. *J. Chem. Phys.* **2006**, *125*, 204710.
- [13] Chapman, W.; Jackson, G.; Gubbins, K. *Mol. Phys.* **1988**, *65*, 1057.
- [14] Sear, R.; Jackson, G. *J. Chem. Phys.* **1996**, *105*, 1113.
- [15] Manoharan, V.; Elsesser, M.; Pine, D. *Science* **2003**, *301*, 483.
- [16] Cho, Y.-S.; Yi, G.-R.; Lim, J.-M.; Kim, S.-H.; Manoharan, V.; Pine, D.; Yang, S.-M. *J. Am. Chem. Soc.* **2005**, *127*, 15968.
- [17] Zerrouki, D.; Rotenberg, B.; Abramson, S.; Baudry, J.; Goubault, C.; Leal-Calderon, F.; Pine, D.; Bibette, J. *Langmuir* **2006**, *22*, 57.
- [18] Zhang, G.; Wang, D.; Möhwald, H. *Angew. Chem. Int. Ed.* **2005**, *44*, 1.
- [19] Mirkin, C.; Letsinger, R.; Mucic, R.; Storhoff, J. *Nature* **1996**, *382*, 607.

- [20] Sear, R. P. *J. Chem. Phys* **1999**, *111*, 4800.
- [21] Lomakin, A.; Asherie, N.; Benedek, G. B. *Proc. Natl. Acad. Sci. U.S.A.* **1999**, *96*, 9465.
- [22] Liu, H.; Kumar, S. K.; Sciortino, F. *J. Chem. Phys.* in press
- [23] Wertheim, M. *J. Stat. Phys.* **1984**, *35*, 19.
- [24] Bianchi, E.; Largo, J.; Tartaglia, P.; Zaccarelli, E.; Sciortino, F. *Phys. Rev. Lett.* **2006**, *97*, 168301.
- [25] Sciortino, F.; Bianchi, E.; Douglas, J. F.; Tartaglia, P. *J. Chem. Phys.* **2007**, *126*, 194903.
- [26] Frenkel, D.; Smit, B. *Understanding Molecular Simulation*; Academic Press: London, 2nd ed., 2001.
- [27] Wilding, N. *Journal of Physics Condensed Matter* **1997**, *9*, 585.
- [28] Romano, F.; Tartaglia, P.; Sciortino, F. *J. Phys.: Condens. Matter* **2007**, *19*, 322101
- [29] Malijevský, A.; Yuste, S.; Santos, A. *J. Chem. Phys.* **2006**, *125*, 074507.

M	Δ	$\cos\theta$	T_c	ρ_c	p_b^c	B_2^c/B_2^{HS}
3	0.050	0.92	0.1076	0.151	0.727	-23.67
3	0.070	0.92	0.1113	0.150	0.732	-24.92
3	0.119	0.92	0.1180	0.134	0.721	-26.71
3	0.119	0.895	0.1252	0.136	0.737	-28.29
3	0.119	0.92	0.1180	0.134	0.721	-26.71
3	0.119	0.95	0.1069	0.131	0.726	-25.13
3	0.119	0.97	0.0968	0.129	0.726	-23.92
4	0.010	0.92	0.1140	0.326	0.656	-4.02
4	0.050	0.92	0.1392	0.306	0.652	-4.32
4	0.070	0.92	0.1468	0.306	0.641	-4.24
4	0.090	0.92	0.1511	0.289	0.642	-4.65
4	0.119	0.92	0.1573	0.276	0.644	-4.92
4	0.119	0.895	0.1682	0.267	0.635	-5.74
4	0.119	0.92	0.1573	0.276	0.644	-4.92
4	0.119	0.94	0.1484	0.307	0.667	-3.85
5	0.010	0.92	0.1259	0.393	0.567	-2.41
5	0.050	0.92	0.1570	0.387	0.588	-2.67
5	0.070	0.92	0.1653	0.374	0.585	-2.81
5	0.090	0.92	0.1723	0.362	0.581	-2.90
5	0.119	0.92	0.1808	0.348	0.577	-3.03
5	0.119	0.895	0.1959	0.333	0.570	-3.53
5	0.119	0.92	0.1808	0.348	0.577	-3.03
5	0.119	0.95	0.1601	0.372	0.589	-2.22

Table 1: Critical point properties for all studied models, labeled by the values M , Δ and $\cos\theta$. The different columns indicate the critical temperature T_c , critical density ρ_c , the bond probability p_b^c and the reduced value of the second virial coefficient B_2^c/B_2^{HS} at the critical point. The estimated errors for each of these quantities are: $\pm 0.0005(T_c)$; $\pm 0.007(\rho_c)$; $\pm 0.005(p_b^c)$. The error in B_2 arises from the error in T_c and differs for each point due to the non-linear relation between B_2 and T . The field-mixing parameter s is always smaller than 0.08.

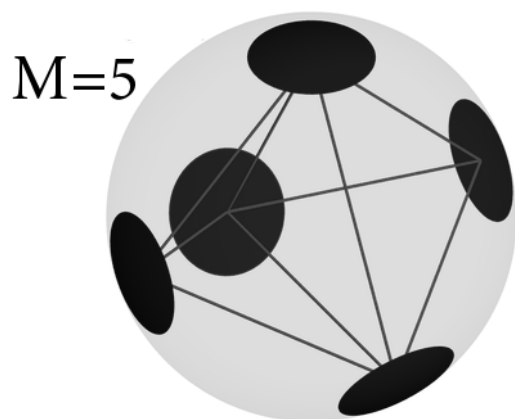
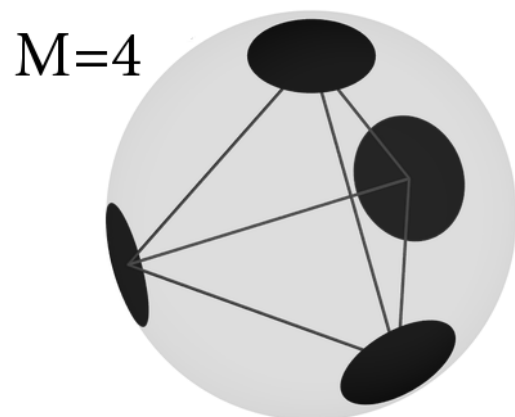
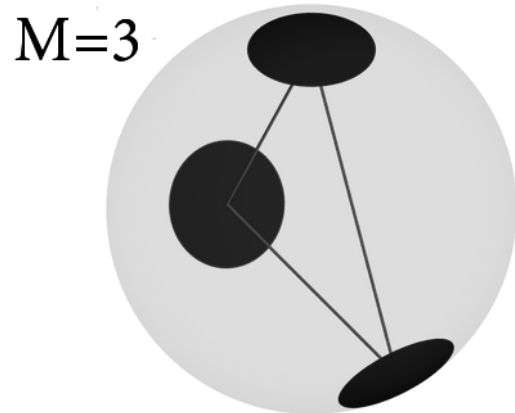


Figure 1: Pictorial representation of the three different patch geometries considered in this work. The solid angle of each patch is $2\pi(1 - \cos \theta)$, where θ is the cone semi-angle.

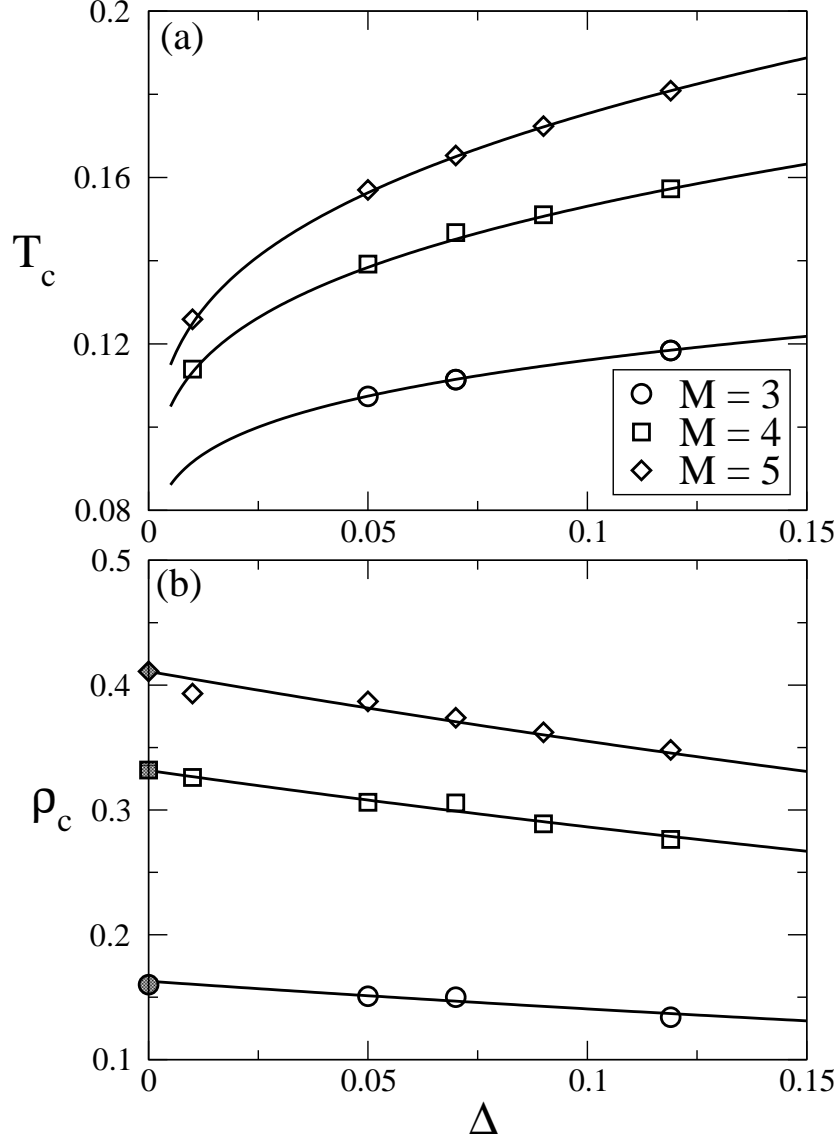


Figure 2: Critical temperature T_c (a) and critical density ρ_c (b) as a function of the range Δ , at fixed patch angular size $\cos \theta = 0.92$. Lines in (a) correspond to constant values of B_2 : specifically $B_2/B_2^{HS} = -3.03$ for $M = 5$, $B_2/B_2^{HS} = -4.92$ for $M = 4$ and $B_2/B_2^{HS} = -26.71$ for $M = 3$. Lines in (b) are $\rho_c(\Delta) = \rho_c(0)/(1 + 0.5\Delta)^3$, where $\rho_c(0)$ (shaded point) is a fitting parameter. The fit values are $\rho_c(0) = 0.41$ for $M = 5$, $\rho_c(0) = 0.33$ for $M = 4$ and $\rho_c(0) = 0.16$ for $M = 3$. Open symbols are simulation results.

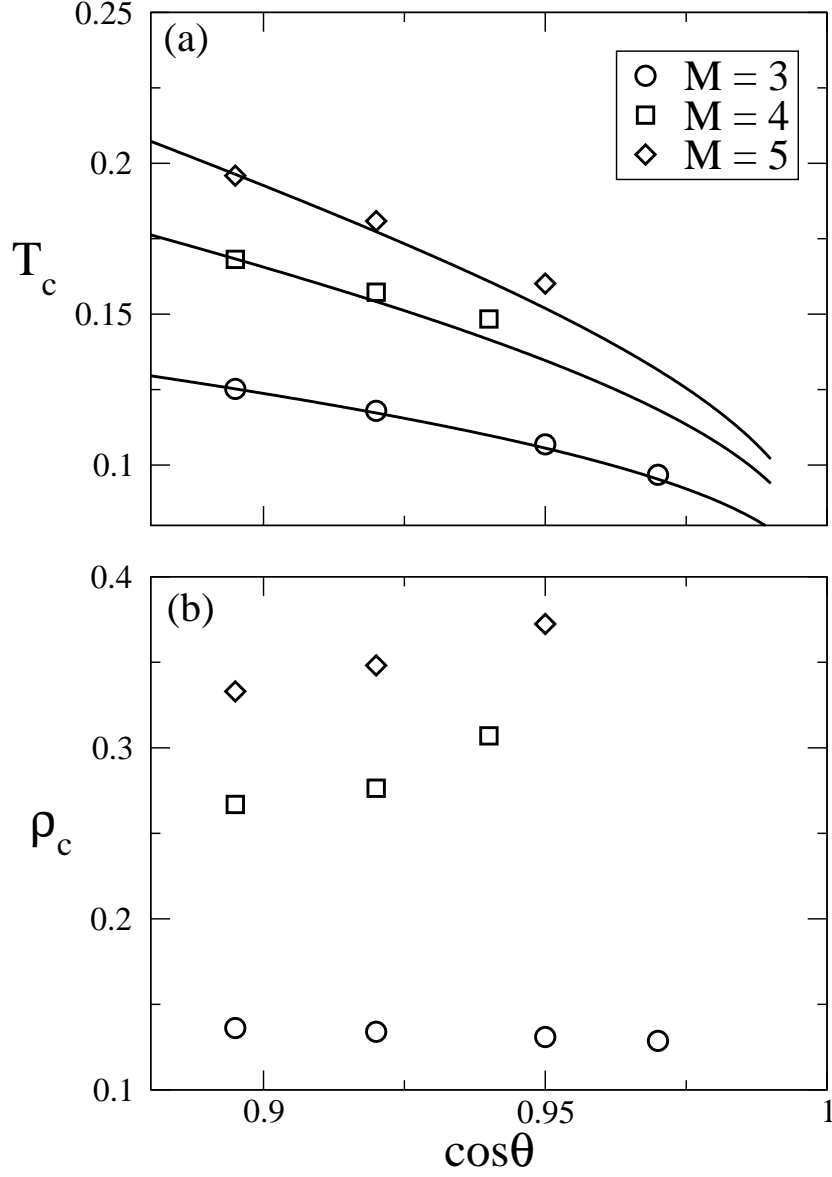


Figure 3: Critical temperature T_c (a) and critical density ρ_c (b) as a function of the angular patch size $\cos\theta$, at fixed range $\Delta = 0.119$. Lines in (a) correspond to constant values of B_2 : specifically $B_2/B_2^{HS} = -3.53$ for $M = 5$, $B_2/B_2^{HS} = -5.74$ for $M = 4$ and $B_2/B_2^{HS} = -28.29$ for $M = 3$. Open symbols are simulation results.